ACS chemical biology

Articles

pubs.acs.org/acschemicalbiology

Degron Protease Blockade Sensor to Image Epigenetic Histone Protein Methylation in Cells and Living Animals

Thillai V. Sekar, Kira Foygel, Rammohan Devulapally, and Ramasamy Paulmurugan*

Molecular Imaging Program at Stanford, Bio-X Program, Stanford University School of Medicine, Stanford, California, United States

Supporting Information

ABSTRACT: Lysine methylation of histone H3 and H4 has been identified as a promising therapeutic target in treating various cellular diseases. The availability of an *in vivo* assay that enables rapid screening and preclinical evaluation of drugs that potentially target this cellular process will significantly expedite the pace of drug development. This study is the first to report the development of a real-time molecular imaging biosensor (a fusion protein, [FLuc2]-[Suv39h1]-[$(G4S)_3$]-[H3-K9]-[cODC]) that can detect and monitor the methylation status of a specific histone lysine methylation mark (H3-K9) in live animals. The sensitivity of this sensor was assessed in various cell lines, in response to down-regulation of methyltransferase EHMT2 by specific siRNA, and in nude mice with lysine replacement mutants. *In vivo* imaging in response to a combination of methyltransferase inhibitors BIX01294 and Chaetocin in mice reveals the potential of this sensor for preclinical drug evaluation. This biosensor thus has demonstrated its utility in the detection of H3-K9 methylations *in vivo* and potential value in preclinical drug development.

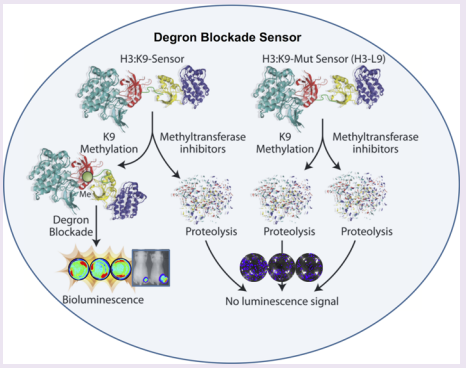

Histone methylation is an important post-translational modification (PTM) that governs chromosome organization and gene regulation in cells. It has been implicated in a spectrum of diseases, such as cancers, intellectual disorders [e.g., fragile X-syndrome (FXS), schizophrenia, depression], neurodegenerative disorders [e.g., Alzheimer's disease and Huntington's disease,[1] heart failure,[2] rheumatoid arthritis (RA),[3] and multiple sclerosis],[4] and aging, and in fact almost all major human disorders. Histone lysine methylation, in particular, has been identified as a "watchdog" that controls the growth and metabolic function of cells in various physiological states. Histone lysine methylation therefore provides promising therapeutic targets due to its regulatory role, and consequently there is significant interest in developing methodologies to screen novel small-molecule drugs capable of modulating this process.

Histone lysine methylation mainly occurs in the N-terminal tail region of histones H3 and H4 in mammalian cells. The collective action of methylation marks along with other epigenetic processes, in particular DNA methylation, controls gene expression and regulates cellular processes. The heterochromatin complex is a region of DNA rich in genes that are silenced via histone methylations. Silenced genes can become transcriptionally active in response to external signaling stimuli.[5] Di- or trimethylations of the H3-K9 mark are prominent post-translational modifications mostly associated with transcriptionally repressive heterochromatin complex and are the main processes involved in X-chromosome inactivation.[6] The interaction of methylated H3-K9 with heterochromatin protein 1 (HP1) is essential for the formation of heterochromatin complexes, which in turn are the essential components for maintaining DNA integrity.[7]

Histone methylations are reversible, and demethylation reactions catalyzed by specific demethylase enzymes are crucial for the reactivation of genes that were previously silenced.[8] Methylation and demethylation reactions at specific histone lysine methylation marks, regulated by a combination of specific methyltransferases and demethylases, are capable of regulating the expression levels of different proteins involved in controlling cellular homeostasis.[9] Therefore, manipulation of gene expression is possible by tuning specific histone methylation marks positioned within H3 and/or H4 histone proteins. Histone H3 has five important lysine methylation marks (H3-K4, H3-K9, H3-K27, H3-K36, and H3-K79) that control chromatin organization and the regulation of gene expression. H4-K20 is the only histone methylation mark identified in histone H4 to date. These methylation marks collectively modulate the transcriptionally active or repressive states of the chromatin complex. H3-K4, H3-K9, and H3-K27 are important methylation marks involved in controlling the expression of key proteins that maintain the pluripotency of embryonic stem cells; for instance, hypermethylation of H3-K4 occurs at the *nanog* gene locus in embryonic stem cells, whereas H3-K4 demethylation occurs at the same gene locus in trophoblast stem cells.[10]

Special Issue: Post-Translational Modifications

Received: October 7, 2014
Accepted: December 9, 2014
Published: December 9, 2014

DOI: 10.1021/cb5008037
ACS Chem. Biol. 2015, 10, 165−174

Degrons are proteasomal recognition sequences present in many proteins that are recognized by the proteasome and thus can direct protein degradation. They are called N- or C-terminal degrons based on their presence on either the N-terminal or C-terminal region of proteins. The C-terminal degron of mouse ornithine decarboxylase (cODC) is a well-studied degron; it induces proteasomal degradation independent of polyubiquitylation. The cODC degron has been utilized for the selective protein degradation of green fluorescent protein (GFP), Ura3 proteins,[11] and several other cellular proteins, including TRAF6 and Rb in experimental research.[12] Additionally, by using the cODC degron, molecular sensors were developed to image the effect of therapeutic radiation-induced cellular 26S proteasome functions[13] and also to track cancer initiating cells (CICs) *in vivo*.[14] Full-length mouse ODC has previously been incorporated at the C-terminal end of green fluorescent protein (GFP)[15] and used for the indirect imaging of cellular protease levels (by measuring the GFP signal). In addition, N-terminal degrons have been used to design sensors for imaging apoptosis, cell death, and cell growth arrest.[16]

The histone methylation status of cultured cells and tissue samples has been routinely detected by various antibody-based assay methods and a few modern spectroscopic assays. Besides these conventional assays, antibody-based strip biosensors have been recently developed to detect histone lysine methylation at specific marks.[17,18] Collectively, aside from the fluorescence-resonance-energy-transfer (FRET) method developed by Lin et al.,[19] all methods reported thus far rely mainly on antibodies that specifically bind to methylated histone proteins. The FRET sensor developed by Lin et al. has demonstrable value in the detection of H3-K9 methylation in mouse embryonic fibroblasts. However, despite the fact that this FRET sensor is able to measure histone methylation effectively, the application of this assay is limited to detection of the histone methylation status in live cells and cannot be used for the real-time *in vivo* monitoring in live animals. To address this issue, we, for the first time, developed a bioluminescence-based molecular biosensor that enables optical bioluminescence imaging of histone methylation status in cell lysates, in intact cells, and in living animals. We adopted the "*degron protease blockade*" as a concept to design our sensor (H3-K9 sensor). To examine the specificity of the H3-K9 methylation sensor, we designed mutant sensors by replacing lysine 9 (K9) with leucine (K9L). Additionally, a sensor protein with mutant Suv39h1 chromodomain was also generated using tryptophan to alanine (W45A) mutation. Our results demonstrate that the developed sensor is robust and sensitive to image H3-K9 methylation in intact cells and in living animals.

RESULTS AND DISCUSSION

Novel Design of H3-K9 Degron Protease Blockade Methylation Sensor. The methylation sensor was designed by combining codon-optimized firefly luciferase (FLuc2), the chromodomain of methyltransferase (Suv39h1: amino acid 42–91), a 15 amino acid linker peptide [$(G_4S)_3$], the first 13 amino acids of the H3 protein (H3-K9: ARTKQTARKSTGG), and the C-terminal 37 amino acid degron of mouse ornithine decarboxylase (cODC). The order of domains from the NH_2 to the COOH terminal are as follows: [FLuc2]-[Suv39h1]-[$(G_4S)_3$]-[H3-K9]-[cODC-Degron]. The H3-L4, H3-L9, and H3-L4L9 mutant sensors were constructed by replacing lysine (K) at methylation marks K9 and K4 of the H3-K9 peptide with leucine (L) (Supporting Information Figure 1). The sensor fusion proteins were expressed under a constitutive CMV promoter in the pcDNA 3.1 (+) vector backbone.

Mouse ODC is the first rate-limiting enzyme in polyamine biosynthetic pathway. In this pathway, polyamines, using a feedback mechanism, promote the degradation of mouse ODC by inducing antizyme. Antizyme, in turn, favors an interaction between 26S proteasome and the C-terminal degron of mouse ODC.[20] Moreover, there are no reports to date that show that degron-proteasomal degradation can be blocked by conformational change mediated by site-specific epigenetic modifications, which occurs within the protein. The present study attempts to evaluate the consequence of interaction between Suv39h1 and the H3-K9 methylation mark. The chromodomain of Suv39h1 specifically interacts with the di- and trimethylated K9 mark of H3 protein. Therefore, the Suv39h1-chromodomain of the sensor interacts with the H3-K9 methylation mark present within the 13 amino acid peptide when it is in the methylated state, resulting in a conformation lock that blocks degron-mediated protein degradation. By contrast, the H3-L9 mutant sensor has an open conformation due to the absence of the [Suv39h1]-[H3-K9] methylation lock (Figure 1). This provides degron access for proteasomal complex, resulting in degradation of the sensor fusion protein by the proteasomal complex, which in turn leads to little or no bioluminescence signal.

Degron-Protease-Blockade Sensor Measures H3-K9 Histone Methylation in Cells. There are six lysine

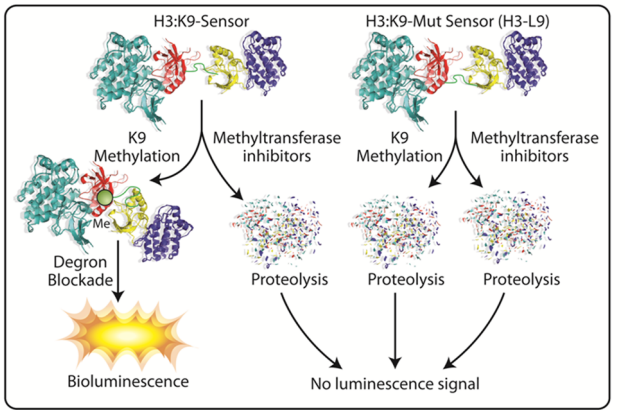

Figure 1. Schematic illustration of the design of degron-protease-blockade histone methylation imaging sensor. The scheme shows the outcome of H3-K9 and its respective mutant (H3-L9) sensor upon methylation by methyltransferase enzymes and in response to the treatment of methyltransferase inhibitors. The sensor is a fusion protein in which a full-length firefly luciferase is fused to H3-K9 peptide, a 15-amino acid linker, Suv39h1-chromodomain, and a 37 amino acid degron protease recognition sequence at the COOH terminal. Upon methylation of the H3-K9 peptide by methyltransferase, the inbuilt Suv39h1 chromodomain is recruited, and this creates a conformational lock that blocks degron-mediated proteasomal degradation of the H3-K9 sensor fusion protein; as a result, intact FLuc protein is accumulated in the cells. By contrast, when histone methyltransferase inhibitors block methylation of the H3-K9 sensor and thereby pave the way for degron-mediated proteasomal degradation of sensor protein, resulting in the loss of FLuc signal. The H3-L9 sensor, which lacks K9 for methylation, undergoes constitutive proteasomal degradation due to the lack of H3-K9–Suv39h1 conformational lock and eventually shows little or no FLuc signal.

DOI: 10.1021/cb5008037
ACS Chem. Biol. 2015, 10, 165–174

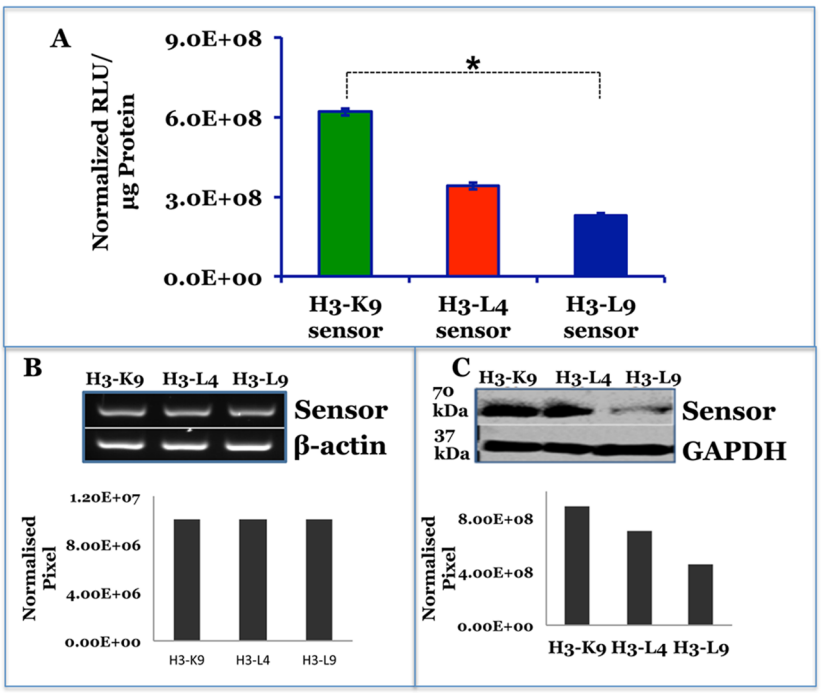

Figure 2. (A) Optical imaging of the degron-protease-blockade histone methylation imaging sensor: (A) Graph showing normalized firefly luciferase signal measured from HepG2-cells transfected with plasmids expressing H3-K9, H3-L4, and H3-L9 degron protease blockade histone methylation sensors. The cells cotransfected with Renilla luciferase expression vector were used for transfection normalization. The samples are in the order as they appear in the *x*-axis labels. Data are mean ± standard error mean of three determinants (*$p < 0.03$). (B) RT-PCR shows the mRNA level of H3-K9, H3-L4, and H3-L9 degron blockade histone methylation sensors, and the graph shows normalized pixel values of DNA bands. (C) Immunoblot shows the level of H3-K9, H3-L4, and H3-L9 degron blockade histone methylation sensors detected with FLuc specific antibody. The lower panel shows the GAPDH protein level, and the graph shows normalized pixel values of sensor protein bands. The experiments were repeated at least a minimum of three times.

methylation marks [H3-K4, H3-K9, H3-K27, H3-K36, H3-K79, and H4-K20] that have been identified within the core histones H3 and H4, which are important for controlling gene expression, and therefore are implicated in diseases like cancer. These six histone lysine methylation marks are thus considered promising therapeutic targets. The lysine molecules located within H3 and H4 are mono-, di-, and tri- methylated by specific methyltransferase enzymes and demethylated by another group of enzymes called demethylases that have only been recently discovered.[8] Most of the current generation drugs targeting histone lysine methylations are designed to inhibit or activate methyltransferase enzymes, rather than directly block or stabilize methylation levels at specific histone lysine methylation marks. Although many drugs are already being screened, their efficacy cannot be ascertained to the fullest extent due to a shortage of histone lysine methylation detection and evaluation methods. To fill these gaps, we developed a real-time methylation-detection optical-imaging biosensor that utilizes a specific interaction between the chromodomain of Suv39h1-histone-lysine *N*-methyltransferase enzyme and H3-K9 methylation mark.

Hepatocellular carcinoma is a primary liver cancer in human, and it has been implicated with deregulation of histone modifications. Epigenetic modifications play a vital role in tumor development, progression, and metastasis. Since this study aims to develop a methylation-imaging sensor with the potential to screen small molecule modulators of histone methylation, we chose HepG2 cells as a primary model for our preliminary evaluation and characterization of degron blockade histone methylation sensor. The suitability of the methylation sensor was initially tested by optical bioluminescence imaging in transfected intact HepG2 cells. Plasmid vectors expressing wild-type (H3-K9) and mutant (H3-L9) methylation sensors were transfected into HepG2 cells after an initial plating of 70 to 80% confluency. H3-K9 methylation mediated firefly luciferase (FLuc) signals were captured at 24 and 48 h post-transfection by 20 min of sequentially imaging with a cooled CCD camera (IVIS), starting immediately after the addition of 50 μg/mL of substrate D-luciferin in PBS. A methylation-specific FLuc signal of $2.5 \times 10^8 \pm 4.1 \times 10^7$ p/s/cm^2/sr was obtained with the wild-type methylation sensor (H3-K9), which is 5.7 ± 0.22 fold higher than what was observed with the K4 mutant (H3-L4) sensor ($4.4 \times 10^7 \pm 1.6 \times 10^6$ p/sec/cm^2/sr), and 11.8 ± 1.1 fold higher than the signal obtained with the K9 mutant (H3-L9) sensor ($2.1 \times 10^7 \pm 1.4 \times 10^6$ p/s/cm^2/sr; Figure 2A).

In order to demonstrate that the luciferase signal generation was due to the methylation-mediated protease blockade, we conducted RT-PCR and immunoblot analysis in transfected cells. Immunoblot was performed on lysates obtained from transfected cells using a FLuc-specific monoclonal antibody. The levels of each sensor protein, detected upon immunoblot analysis, were correlated with the luciferase signal obtained from the respective sensor, whereas the mRNA levels of all three sensors remained the same (Figure 2B,C). This indicates that the wild-type sensor is resistant to proteolytic cleavage due to a methylation-mediated conformational blockade that disables recognition of the degron sequence by the proteasome, whereas mutant sensors with a flexible open conformation remain susceptible to proteolytic cleavage. To evaluate

DOI: 10.1021/cb5008037
ACS Chem. Biol. 2015, 10, 165−174

specificity, we also constructed methylation sensors with a tryptophan to alanine (W45A) mutation in the Suv39h1 chromodomain in both the H3-K9 sensor and the H3-L9 sensor. Both were evaluated in transfected HepG2 cells. A significant drop in luciferase signal ($p < 0.01$) was observed in cells expressing either the sensor protein containing mutant chromodomain or mutations in both the chromodomain and interaction domain, in comparison to cells expressing the wild-type counterparts (Supporting Information Figure 2A).

Degron-Protease-Blockade Sensor Expressed with Nuclear Localization Signal (NLS) Sequence. Because histone methylation is a nuclear event, we tested whether additional NLS, in addition to the inherent NLS located in the chromodomain of the sensor, is needed in localizing the sensor to the nucleus and enhancing methylation signal. We tested the methylation-mediated bioluminescence signal by introducing NLS at the C-terminus of the sensor fusion protein. Moreover, the addition of NLS signal peptide downstream from degron allowed us to test whether the NLS sequence has any impact on the recognition of degron sequence by protease in the degradation process. The degron-protease-blockade-methylation sensor with NLS in the C-terminal end was tested in HepG2 cells. The luciferase signals measured in HepG2 cells, which were transfected with methylation sensors with or without NLS sequence, showed that the addition of NLS sequence at the C-terminal end of the degron-protease-methylation sensor did not have any significant effect on the observed bioluminescence signal (Supporting Information Figure 2B), and the fold variation between the wild-type and the mutant sensors, with or without NLS, remained unchanged. The H3-K9 sensor with the NLS tag yielded a luciferase signal of $3.35 \times 10^7 \pm 3.06 \times 10^6$ RLU/μg protein, whereas the H3-K9 sensor with no NLS tag gave a luciferase signal of $3.32 \times 10^7 \pm 3.02 \times 10^6$ RLU/μg protein. These results clearly demonstrate that the chromodomain of Suv39h1 and the first 13 amino acids of H3 proteins, which harbor inherent nuclear localization signals, are sufficient to localize the methylation sensors to the nucleus, facilitating methyltransferase enzyme action.

Mutant-FRB (FRB*) In a Degron Mimetic to Modulate Histone Methylation Sensor by Rapamycin. As an attempt to modulate histone methylation-mediated bioluminescent signal by our protease blockade sensor, we constructed a methylation sensor that contained a triple mutant form of FKBP12 rapamycin binding protein (FRB*) in place of the cODC degron as a degron mimetic. This FRB-triple mutant (K2095P, T2098L, and W2101F) has previously been used as a protein degradation initiator, including glycogen synthase kinase-3 (GSK-3β), glutathione S-transferase (GST), and firefly luciferase;[21,22] therefore its addition to the C-terminal end of the unmethylated sensor was expected to degrade the fusion protein. The binding of rapamycin to FRB* alters the conformational switch and can prevent the recognition of FRB* by a protease independent of methylation blockade. Hence, this system can be modulated in two ways. We imaged the wild-type and mutant sensors constructed with the FRB* sequence in HepG2 cells before and after modulation with rapamycin. The results showed a significant increase ($p = 0.0002$) in bioluminescent signal when cells expressing the H3-K9 sensor were treated with 40 nM of rapamycin. However, there was no change in the bioluminescence signal measured in cells expressing the mutant sensor (H3-L9) with or without the addition of rapamycin. Immunoblot analysis of cell lysates obtained from HepG2 cells transfected with either wild-type or mutant sensors, with or without rapamycin treatment, demonstrated a good correlation between sensor protein levels and the luciferase signal measured using optical imaging (Supporting Information Figure 3A–C). These results show that sensors containing the FRB* degron sequence are less efficient than those containing the cODC degron sequence in terms of protease recognition.

The Degron-Protease-Blockade Sensor Is Capable of Measuring H3-K9Methylation in Different Cells. The ability of the H3-K9 degron-protease-blockade-methylation sensor to detect histone lysine methylations was evaluated not only in HepG2 cells but also in MDA-MB231, HEK293T, and MCF7 cells, in order to determine the generalizability of the sensor in various types of cells. The cells transfected with the H3-K9 methylation sensor showed significantly higher levels of luciferase signal (HepG2: $2.5 \times 10^8 \pm 2.3 \times 10^7$ p/s/cm^2/sr; MDA-MB231: $8.38 \times 10^6 \pm 2.1 \times 10^6$ p/s/cm^2/sr; HEK293T: $8.2 \times 10^7 \pm 2.7 \times 10^7$ p/s/cm^2/sr; MC7: $7.1 \times 10^7 \pm 6.1 \times 10^6$ p/s/cm^2/sr) compared to mutant sensors (H3-L9 and H3-L4L9) in all four cell lines. The fold variation of luciferase signals between wild-type and K9 mutant (H3-L9) sensors in HepG2, MDA-MB231, HEK293T, and MCF7 cells were 5.7, 4.29, 6.65, and 9.22, respectively, whereas signal fold variations between the wild-type and double mutant sensors (H3-L4L9) were 11.85, 50.96, 11.73, and 35.78, respectively (Supporting Information Figure 4A–D). The expression level of endogenous methyltransferase EHMT2, which is predominantly responsible for the methylation of the H3-K9 peptide, was tested using immunoblot to correlate the sensor signal. The levels of EHMT2 methyltransferase protein observed in these cells correlated with methylation-mediated luciferase signals recorded (Supporting Information Figure 5A–C). However, luciferase signals measured in HepG2 cells were higher than the EHMT2 protein level detected in these cells, which suggests the presence of other methyltransferase enzymes capable of catalyzing the H3-K9 methylation mark.[23] These results clearly demonstrate that the degron-blockade-methylation sensor is sufficiently generalizable, specific, and sensitive to image H3-K9 methylation in different cell types, and while the absolute level of signal varies among cell lines, the fold changes between the wild-type and the mutant sensors remain consistent across different cell lines.

The Degron-Protease-Blockade Sensor Measures H3-K9Methylation Modulated by Methyltransferase (MT) Inhibitors. After determining the potential of the degron-protease-blockade-methylation sensor in measuring H3-K9 methylation in different types of cells, we further tested the specificity of the sensor in response to drugs that alter the level of endogenous methyltransferase enzymes. The inhibition of methyltransferase enzymes indirectly led to the reduction in the level of methylation of specific histone methylation marks. We used MT inhibitors, such as BIX01294, a specific inhibitor of EHMT2; UNC0638, a specific inhibitor of EHMT2, GLP, SET7/9, and SET8; and Chaetocin, a mycotoxin which selectively inhibits SU(VAR)3–9, EHMT2, DIM5, EZH2, and SET7/9 methyltransferase enzymes. To show the specificity of the degron-blockade-methylation sensor, we used various concentrations of BIX01294, UNC0638, and Chaetocin to assess luciferase activity. BIX01294 at concentrations of 0, 0.5, 1, 2, 3, and 4 μM was delivered to HepG2 cells stably expressing the H3-K9 methylation sensor or its mutant (H3-L9) counterpart, and a luciferase assay was

DOI: 10.1021/cb5008037
ACS Chem. Biol. 2015, 10, 165–174

performed to assess the effects. Methylation-mediated-luciferase-signal was proportionately reduced in response to the increase in the concentration of BIX01294 in cells expressing the H3-K9 sensor, whereas no significant signal change was observed in cells expressing the mutant sensor (Figure 3A).

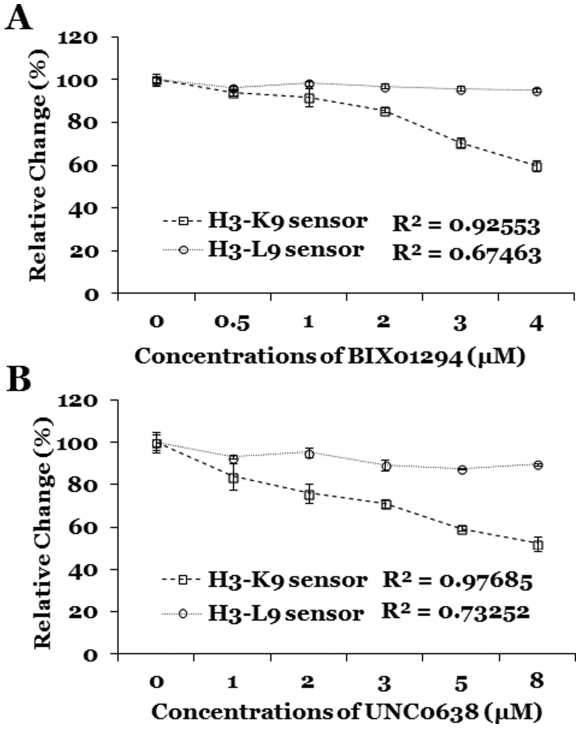

Figure 3. Degron protease blockade histone methylation imaging sensors in response to different concentration of methyltransferase inhibitors (BIX01294 and UNC0638) studied in HepG2 cells stably expressing the sensors. (A) Firefly luciferase signal measured from stable HepG2 cells expressing H3-K9 and H3-L9 sensors exposed to various concentrations (0 to 4.0 μM) of BIX01294. (B) Firefly luciferase signal measured from stable HepG2 cells expressing H3-K9 and H3-L9 sensors exposed to various concentrations (0 to 8.0 μM) of UNC0638. Data are mean ± standard error mean of three determinants.

Similarly, UNC0638 and chaetocin were tested at concentrations of 0, 1, 2, 3, 5, and 8 μM and 0, 0.1, 0.2, 0.4, 0.6, and 0.8 μM, respectively. The measured luciferase-enzyme signal was inversely proportional to the concentrations of UNC0638 (Figure 3B) and chaetocin (Figure 4A) used for the study. In addition, we also evaluated methylation-mediated-luciferase signal in response to the treatment of combination of chaetocin and BIX01294 (0.1 μM chaetocin +0.5, 1.0, 1.5, 2.0, and 3.0 μM BIX01294) and, chaetocin and UNC0638 (0.1 μM chaetocin +0.5, 1.0, 2.0, 3.0, and 4.0 μM UNC0638) in HepG2 cells stably expressing the H3-K9 sensor. A dose-dependent reduction in luciferase signal was observed in cells expressing the H3-K9 sensor (Figure 4B,C). Chaetocin treatment at a concentration above 0.4 μM caused significant toxicity.

Additionally, we also tested the effect of an inhibitor of the demethylase enzyme on endogenous H3-K9 methylation and H3-K9 methylation sensor signal. The HepG2 cells stably expressing the H3-K9 sensor was treated with JIB-04 at various concentrations (0 to 600 nM) and measured for a sensor signal by luciferase assay. The results showed a JIB-04 concentration dependent increase in luciferase signal. The result was compared with sensor signals measured in cells treated with various concentrations of MT inhibitor BIX01294 (0−5 μM). The BIX01294 showed a concentration dependent decrease in the luciferase signal while JIB-04 was showing a concentration dependent increase (R^2 = 0.9549 for BIX01294, R^2 = 0.7881 for JIB-04; Figure 5). The immunoblot analysis of cells for endogenous dimethylated H3-K9 protein showed a good correlation with the luciferase signal.

SiRNA-Mediated Silencing of EHMT2Methyltransferase Expression Confirms the Specificity of Degron-Protease-Blockade Sensor in Measuring H3-K9Methylation. EHMT2 is a methyltransferase enzyme predominantly responsible for the dimethylation of the H3-K9 methylation mark. To test whether EHMT2 methyltransferase is involved in methylating the expressed H3-K9 sensor fusion protein in a manner similar to what has been observed in the endogenous H3-K9 mark, we selectively silenced the EHMT2 methyltransferase level by siRNA. We transfected an EHMT2-specific siRNA-pool into HepG2 cells stably expressing the methylation sensor and performed a luciferase assay and immunoblot analysis of cell lysates. Blockade of EHMT2 expression resulted in an 0.6-fold reduction in methylated sensor protein levels and luciferase signal compared to HepG2 cells treated with the scrambled siRNA counterpart (Figure 6A−C). These results demonstrated a correlation between the methylation status of the H3-K9 peptide in the fusion protein, sensor signaling, and the level of EHMT2 methyltransferase expression.

The Degron-Blockade Histone Methylation Sensor Isolated from Active Chromatin Complex Highlights its Functional Similarity with the Endogenous K9Methylated H3 Protein. To confirm that the methylated wild-type (H3-K9) sensor behaves like an endogenous K9-methylated H3 core protein, we extracted proteins from the histone fraction (DNA bound) and histone-free fraction and performed an immunoblot analysis using a FLuc-specific antibody. The H3-K9 methylation-sensor protein was coeluted with histone protein fraction, whereas the H3-L9 (mutant) sensor protein was coeluted with the cytoplasmic (histone-free) fraction. These results demonstrated a protein−DNA interaction between the methylated H3-K9 domain and the heterochromatin complex, whereas the mutant sensor was independent of heterochromatin due to the unmethylated state of the H3-L9 domain (Figure 6D).

Imaging H3-K9 Histone Methylation Mark in Living Animals by Degron-Protease-Blockade Sensor. The results from *in vitro* experiments clearly show that the H3-K9-degron-protease-blockade-methylation sensor provides a specific and sensitive method of measuring histone methylation in various cells. To further demonstrate utility, we attempted to examine the *in vivo* imaging potential of the histone methylation sensor in small animal model, which is standard for the preclinical evaluation of small molecule drugs in various cellular targets. We chose a nude mice model to generate a luciferase signal with less light attenuation for efficient optical bioluminescence imaging. A tumor xenograft of HepG2 cells was generated by subcutaneous implantation of HepG2 cells stably coexpressing Renilla luciferase-mRFP (RLuc-mRFP) and either the H3-K9 (wild-type) or H3-L9 (mutant) sensors on the lower flank of nude mice. Bioluminescence imaging was performed using the IVIS spectrum optical imaging system once the tumors reached 2−3 mm in diameter (2 weeks after implantation). The methylation-mediated FLuc signal obtained

DOI: 10.1021/cb5008037
ACS Chem. Biol. 2015, 10, 165−174

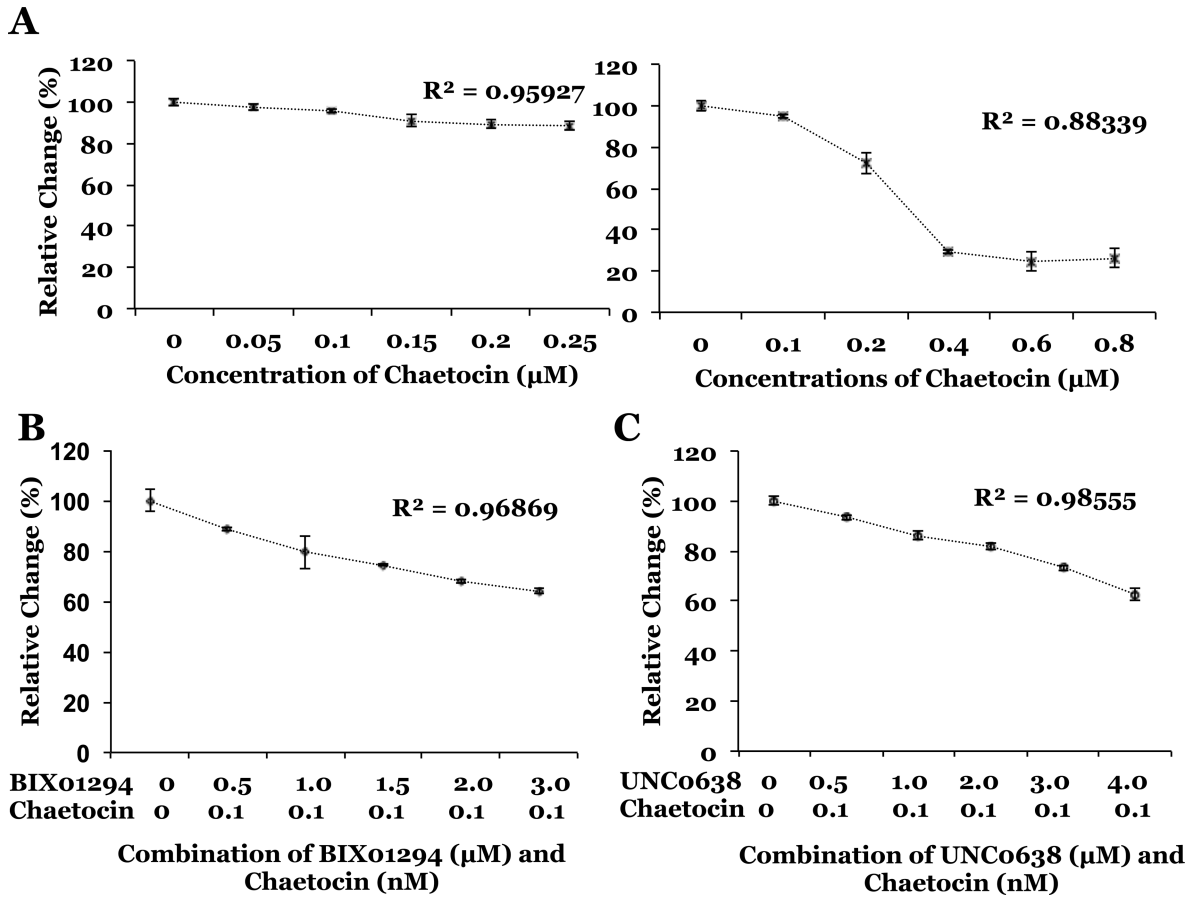

Figure 4. H3-K9 imaging sensor in response to different concentrations of methyltransferase inhibitor (Chaetocin, BIX01294, and UNC0638) studied in HepG2 cells stably expressing the H3-K9 sensor. (A) Firefly luciferase signal measured from stable HepG2 cells expressing the H3-K9 sensor exposed to various concentrations (0 to 0.25 μM and 0 to 0.8 μM) of Chaetocin. Concentrations of drugs are labeled on the *x*-axis. (B) Firefly luciferase signal measured from stable HepG2 cells expressing the H3-K9 sensor exposed to 0.1 μM chaetocin with different concentrations (0 to 3.0 μM) of BIX01294. (C) Firefly luciferase signal measured from HepG2 cells stably expressing the H3-K9 sensor exposed to 0.1 μM chaetocin with various concentrations (0 to 4.0 μM) of UNC0638. Concentrations of drugs are labeled on the *x*-axis. Data are mean ± standard error mean of three determinants.

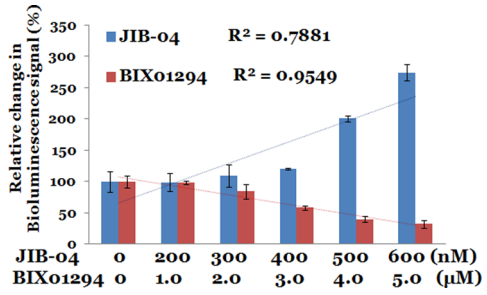

Figure 5. H3-K9 imaging sensor in response to methyltransferase and demethylase inhibitors (BIX01294 and JIB-04) studied in HepG2 cells stably expressing the H3-K9 sensor. Graph showing normalized luciferase signals in HepG2 cells stably expressing the H3-K9 sensor treated with various concentrations of BIX01294 and JIB-04. Concentrations of drugs are labeled on the *x*-axis. Data are mean ± standard error mean of three determinants.

from tumors expressing the H3-K9 wild-type methylation sensor (normalized to tumor volume) was 3.1 ± 0.7 fold higher than the signal obtained from tumors expressing the H3-L9 mutant sensor (0.8 ± 0.3; Figure 7A,B).

On a side note, we observed that while HepG2 cells expressing the mutant sensor (H3-L9) showed equal and consistent growth patterns with the cells expressing the wild-type sensor in cell culture, there was a marked difference in tumor growth when these cells were implanted in animals. In 12 of 15 animals, tumors generated from cells expressing the mutant sensor grew to less than 1 mm in diameter, while tumors generated from cells expressing the wild-type sensor reached 5 mm in diameter.

To further demonstrate the value of the sensor in the screening of small molecules that target histone lysine methylations, tumor-bearing nude mice were treated with a combination of chaetocin (0.2 mg/kg) and BIX01294 (20 mg/kg) every other day for 6 days, and imaging was done every day for 12 days. Significant reduction in luciferase signal was seen in mice treated with this combination of drugs (Figure 7C,D). Mice treated with chaetocin and BIX01294 showed a 2.05 ± 0.3 fold luciferase signal reduction between day 3 ($9.0 \times 10^6 \pm 2.4 \times 10^5$) and day 8 ($3.6 \times 10^6 \pm 8.5 \times 10^5$). The results presented thus far clearly show that the degron-protease-blockade-methylation sensor is sensitive and specific enough to enable imaging of histone methylation marks, both in cells and in small animals, and is suitable for preclinical evaluation of small molecule inhibitors capable of modulating the methylation of histone proteins at specific lysine residues.

DOI: 10.1021/cb5008037
ACS Chem. Biol. 2015, 10, 165−174

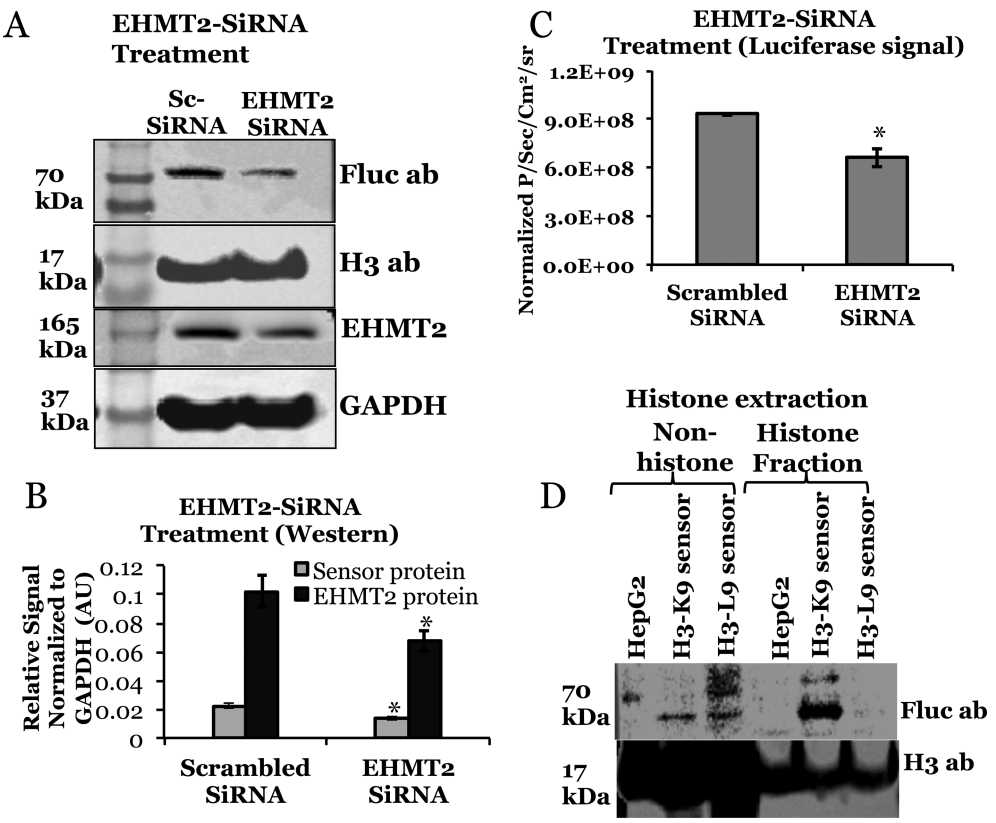

Figure 6. EHMT2 specific SiRNA blocks dimethyl H3-K9 methylation. (A) Immunoblot analysis shows the protein level of the H3-K9 sensor (FLuc ab), endogenous H3, EHMT2, and GAPDH in HepG2 cells stably expressing the H3-K9 sensor treated with scrambled and EHMT2-specific SiRNA. (B) Graph shows the relative normalized signal of the H3-K9 sensor and EHMT2 proteins in SiRNA-treated HepG2 cells stably expressing the H3-K9 sensor. (C) Graph showing normalized luciferase signals in HepG2 cells stably expressing the H3-K9 sensor treated with scrambled and EHMT2-specific SiRNA. (D) Immunoblot shows the H3-K9 and H3-L9 sensors copurified with histone fractions and nonhistone fractions of HepG2 cells stably expressing H3-K9 and H3-L9 sensors and detected with a FLuc specific antibody. Lower panel shows histone H3 protein.

The screening and preclinical evaluation of small-molecule drugs targeting histone modifications need to be validated in small animals before proceeding further for toxicological studies, and then on to clinical trials. To the best of our knowledge, currently there is no real-time *in vivo* imaging method available to detect histone methylation status of a specific histone lysine methylation mark in living animals. The degron blockade sensor described in the present study has enabled efficient measurement of the status of H3-K9-methylation mark via optical bioluminescence imaging of xenografts in living animals. In addition, histone methylation imaging of the tumor response to MT inhibitors in nude mice demonstrated the potential of this sensor in drug response evaluation in small animals. The degron-protease-blockade-methylation sensor described in the present study therefore is suitable for histone methylation based drug screening, *in vitro* validation, and preclinical evaluation in small animals, all in one system.

The Degron-Protease-Blockade Histone Methylation Sensor Clearly Distinguishes the Endogenous H3-K9Methylation Status of Human Induced Pluripotent Stem Cells (hiPSC) and Differentiated Embryoid Bodies (EBs). Dimethylated H3-K9 is expressed differentially in embryonic stem cells, hiPSCs, and differentiated stem cells. Patterns of H3-K9 and H3-K27 trimethylation dramatically change during the conversion of an embryonic stem cell to lineage-committed cells, and the blockage of trimethyl H3-K9 and H3-K27 marks is especially expanded in fibroblasts.[24] A sensitive imaging sensor would, in theory, be able to distinguish the differential expression of specific histone methylation marks. Therefore, the suitability of the degron-protease-blockade-histone-methylation sensor in detecting the methylation status of H3-K9 was validated in hiPSCs and differentiated embryoid body (EB) cells. The methylation status of H3-K9 in hiPSCs and EB cells was determined by transfecting them with vectors expressing the H3-K9 and H3-L9 sensors in 12-well plates, followed by a luciferase assay performed 24 h post transfection. A luciferase signal of 3.5×10^4 RLU/μg protein was obtained from EB cells transfected with the H3-K9 sensor, which was significantly (~2 fold) higher than (1.7×10^4 RLU/μg protein) the same sensor transfected in hiPSCs (Figure 8A). The luciferase signal was significantly lower in hiPSCs and EB cells transfected with the H3-L9 sensor compared to the respective cells transfected with the H3-K9 sensor. The luciferase signal obtained from hiPSCs and EB cells that were transfected with the H3-K9 sensor correlated well with the levels of endogenous dimethylated H3 protein at the H3-K9 mark, assessed in respective cells by immunoblot analysis (Figure 8B). These results were well corroborated with previous reports, which showed that H3-K9 methylation is significantly lower in stem cells and hiPSCs when compared to their respective differentiated lineages,[25] and the observations of higher large organized chromatin dimethylated H3-K9 modified regions (LOCKs) in differentiated embryonic stem cells (31%) when compared to undifferentiated mouse embryonic stem cells (~4%).[26]

DOI: 10.1021/cb5008037
ACS Chem. Biol. 2015, 10, 165−174

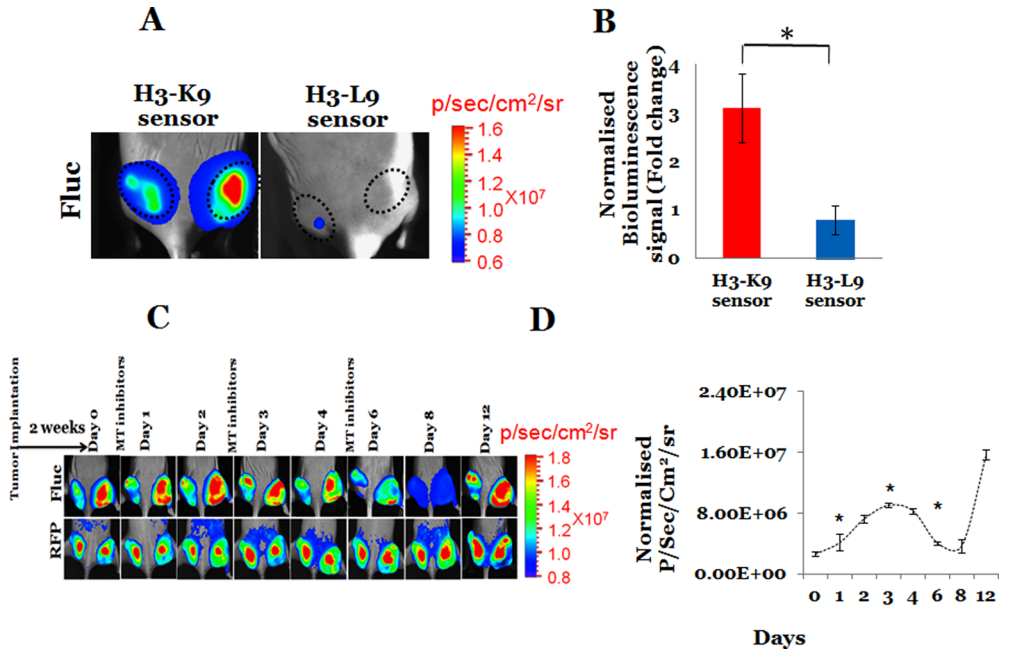

Figure 7. Degron blockade histone methylation in small animal model. (A) Image shows firefly luciferase signals measured from HepG2 xenografts expressing H3-K9 and H3-L9 sensors. (B) Quantitative graph showing normalized luciferase signals recorded in a HepG2 xenograft expressing H3-K9 and H3-L9 sensors (*$p < 0.001$). (C) Firefly luciferase (FLuc) and Red fluorescent protein (RFP) signals of HepG2 xenografts expressing the H3-K9 sensor imaged in different day intervals. The animals were treated with a combination of methyltransferase (MT) inhibitors (Chaetocin and BIX01294) and imaged at different time intervals. (D) Quantitative graph showing normalized luciferase signal measured at different day intervals from the HepG2 xenograft expressing the H3-K9 sensor treated with MT inhibitors (Chaetocin + BIX01294). (*) Indicates time point of drug injection.

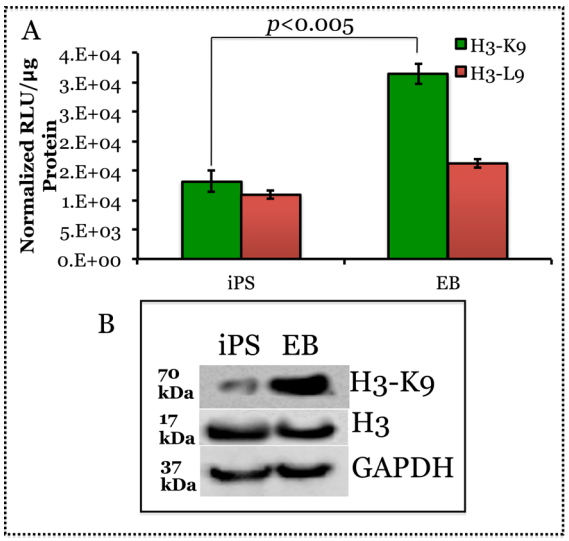

Figure 8. Imaging histone H3-K9 methylation in hiPSC and differentiated EB. (A) Firefly luciferase signals measured from hiPSCs and embryoid bodies (EBs) transfected with plasmids expressing H3-K9 and H3-L9 sensors. (B) Immunoblot shows the level of dimethyl H3-K9, H3 protein, and GAPDH in hiPSCs and EBs.

H3-K9 methylation is identified as an epigenetic determinant of pre-iPSCs, and the removal of H3-K9 methylation leads to fully reprogrammed iPSCs. Furthermore, knockdown of the setdb1 gene (that encodes histone-lysine *N*-methyltransferase) has been shown to induce the reprogramming of pre-iPSCs to iPSCs.[27] Genome-wide remodeling of H3-K9 methylation has been implicated in the transition of embryonic stem cells to mesenchymal-like cells and ascorbic acid (vitamin C)-mediated reduction of H3-K9 methylation-induced transition of mesenchymal-like cells to embryonic stem cells.[28] iPSC generation is a milestone in regenerative medicine, and research efforts are underway to understand the epigenetic mechanism in iPSC formation and to find factors that control epigenetic modifications. Our findings demonstrate that the degron-blockade-histone-methylation sensor, which can sensitively measure the methylation status of hiPSC cells and differentiated cell lineages (i.e., embryoid bodies), will expedite epigenetic studies in stem cell research in the future. However, the current design of our sensor is not capable of detecting the exact degree of methylation, such as that seen in mono-, di-, and tri-methylation for the H3-K9 mark. We are currently looking for chromodomains from interaction partners that can specifically bind to one of these three modifications that are more specifically designed for independent sensors, capable of sensitively measuring mono-, di-, and tri- methylation of various histone methylation marks.

Conclusion. In summary, in this study we have developed a methylation sensor to image the dynamics of methylation in the H3-K9 mark. Its operation relies on degron protease blockade by methylation in the H3-K9 mark. The compelling evidence presented in this report demonstrates the power of the degron-blockade-methylation-imaging sensor for real-time monitoring of histone methylation in various cells as well as xenografts generated in small living animals. The degron-blockade-methylation sensor is sensitive and specific enough to image dimethylation flux of the H3-K9 mark. It is capable of detecting methylation modulation in response to different methyltransferase and demethylase inhibitors in intact cells and small animals. Overall, this imaging sensor will pave the way for the development of novel small molecule drugs targeting the H3-K9 methylation mark. By replacing the 13 amino acid peptide

DOI: 10.1021/cb5008037
ACS Chem. Biol. 2015, 10, 165−174

and interacting domain, this sensor could be used to image other important histone lysine methylation marks. However, further studies that test various other interaction partners and histone methylation domains (H3-K4, H3-K27, H3-K36, H3-K79, and H4-K20) will be required to ascertain the generalizability of the protease blockade sensor.

METHODS

Refer to the Supporting Information for methods. All experiments were repeated a minimum of three times with triplicate samples at each time.

ASSOCIATED CONTENT

Supporting Information

Supplementary figures, materials, and methods. This material is available free of charge via the Internet at http://pubs.acs.org.

AUTHOR INFORMATION

Corresponding Author

*Phone: 650-725-6097 Fax: 650-721-6921 Email: paulmur8@stanford.edu.

Notes

The authors declare no competing financial interests.

ACKNOWLEDGMENTS

We gratefully acknowledge the constant support and encouragement rendered by Dr. S Gambhir, Chair, Department of Radiology, and Stanford University School of Medicine. We thank Department of Radiology, Stanford University School of Medicine, and NIH-NCI RO1CA161091 (R. Paulmurugan) for funding support and Canary Center at Stanford, Department of Radiology for facility and resources. We would like to acknowledge Dr. H Nejadnik and Dr. H. E. Daldrup-Link for providing hiPSC cells. We thank Dr. A. Sheahan for her time in proof reading the manuscript.

REFERENCES

(1) Jarome, T. J., and Lubin, F. D. (2013) Histone lysine methylation: critical regulator of memory and behavior. *Rev. Neurosci. 24*, 375−387.

(2) Papait, R., Greco, C., Kunderfranco, P., Latronico, M. V., and Condorelli, G. (2013) Epigenetics: a new mechanism of regulation of heart failure? *Basic Res. Cardiol. 108*, 361.

(3) Viatte, S., Plant, D., and Raychaudhuri, S. (2013) Genetics and epigenetics of rheumatoid arthritis. *Nat. Rev. Rheumatol. 9*, 141−153.

(4) Huynh, J. L., and Casaccia, P. (2013) Epigenetic mechanisms in multiple sclerosis: implications for pathogenesis and treatment. *Lancet Neurol. 12*, 195−206.

(5) Jenuwein, T., and Allis, C. D. (2001) Translating the histone code. *Science 293*, 1074−1080.

(6) Lachner, M., O'Sullivan, R. J., and Jenuwein, T. (2003) An epigenetic road map for histone lysine methylation. *J. Cell Sci. 116*, 2117−2124.

(7) Richards, E. J., and Elgin, S. C. (2002) Epigenetic codes for heterochromatin formation and silencing: rounding up the usual suspects. *Cell 108*, 489−500.

(8) Anand, R., and Marmorstein, R. (2007) Structure and mechanism of lysine-specific demethylase enzymes. *J. Biol. Chem. 282*, 35425−35429.

(9) Albert, M., and Helin, K. (2010) Histone methyltransferases in cancer. *Semin. Cell Dev. Biol. 21*, 209−220.

(10) Hattori, N., Imao, Y., Nishino, K., Ohgane, J., Yagi, S., Tanaka, S., and Shiota, K. (2007) Epigenetic regulation of Nanog gene in embryonic stem and trophoblast stem cells. *Genes Cells 12*, 387−396.

(11) Hoyt, M. A., Zhang, M., and Coffino, P. (2003) Ubiquitin-independent mechanisms of mouse ornithine decarboxylase degradation are conserved between mammalian and fungal cells. *J. Biol. Chem. 278*, 12135−12143.

(12) Matsuzawa, S., Cuddy, M., Fukushima, T., and Reed, J. C. (2005) Method for targeting protein destruction by using a ubiquitin-independent, proteasome-mediated degradation pathway. *Proc. Natl. Acad. Sci. U. S. A. 102*, 14982−14987.

(13) Brush, J. M., Kim, K., Sayre, J. W., McBride, W. H., and Iwamoto, K. S. (2009) Imaging of radiation effects on cellular 26S proteasome function in situ. *Int. J. Radiat. Biol. 85*, 483−494.

(14) Vlashi, E., Kim, K., Lagadec, C., Donna, L. D., McDonald, J. T., Eghbali, M., Sayre, J. W., Stefani, E., McBride, W., and Pajonk, F. (2009) In vivo imaging, tracking, and targeting of cancer stem cells. *J. Natl. Cancer Inst. 101*, 350−359.

(15) Momose, I., Tatsuda, D., Ohba, S., Masuda, T., Ikeda, D., and Nomoto, A. (2012) In vivo imaging of proteasome inhibition using a proteasome-sensitive fluorescent reporter. *Cancer Sci. 103*, 1730−1736.

(16) Xie, J., Wang, C., Virostko, J., Manning, H. C., Pham, W., Bauer, J., and Gore, J. C. (2013) A novel reporter system for molecular imaging and high-throughput screening of anticancer drugs. *Chembiochem 14*, 1494−1503.

(17) Zeng, W., de Greef, J. C., Chen, Y. Y., Chien, R., Kong, X., Gregson, H. C., Winokur, S. T., Pyle, A., Robertson, K. D., Schmiesing, J. A., Kimonis, V. E., Balog, J., Frants, R. R., Ball, A. R., Jr., Lock, L. F., Donovan, P. J., van der Maarel, S. M., and Yokomori, K. (2009) Specific loss of histone H3 lysine 9 trimethylation and HP1gamma/cohesin binding at D4Z4 repeats is associated with facioscapulohumeral dystrophy (FSHD). *PLoS Genet. 5*, e1000559.

(18) Ge, C., Yu, L., Fang, Z., and Zeng, L. (2013) An enhanced strip biosensor for rapid and sensitive detection of histone methylation. *Anal. Chem. 85*, 9343−9349.

(19) Lin, C. W., Jao, C. Y., and Ting, A. Y. (2004) Genetically encoded fluorescent reporters of histone methylation in living cells. *J. Am. Chem. Soc. 126*, 5982−5983.

(20) Pegg, A. E. (2006) Regulation of ornithine decarboxylase. *J. Biol. Chem. 281*, 14529−14532.

(21) Stankunas, K., Bayle, J. H., Gestwicki, J. E., Lin, Y. M., Wandless, T. J., and Crabtree, G. R. (2003) Conditional protein alleles using knockin mice and a chemical inducer of dimerization. *Mol. Cell 12*, 1615−1624.

(22) Stankunas, K., Bayle, J. H., Havranek, J. J., Wandless, T. J., Baker, D., Crabtree, G. R., and Gestwicki, J. E. (2007) Rescue of degradation-prone mutants of the FK506-rapamycin binding (FRB) protein with chemical ligands. *Chembiochem 8*, 1162−1169.

(23) Fritsch, L., Robin, P., Mathieu, J. R., Souidi, M., Hinaux, H., Rougeulle, C., Harel-Bellan, A., Ameyar-Zazoua, M., and Ait-Si-Ali, S. (2010) A subset of the histone H3 lysine 9 methyltransferases Suv39h1, G9a, GLP, and SETDB1 participate in a multimeric complex. *Mol. Cell 37*, 46−56.

(24) Hawkins, R. D., Hon, G. C., Lee, L. K., Ngo, Q., Lister, R., Pelizzola, M., Edsall, L. E., Kuan, S., Luu, Y., Klugman, S., Antosiewicz-Bourget, J., Ye, Z., Espinoza, C., Agarwahl, S., Shen, L., Ruotti, V., Wang, W., Stewart, R., Thomson, J. A., Ecker, J. R., and Ren, B. (2010) Distinct epigenomic landscapes of pluripotent and lineage-committed human cells. *Cell Stem Cell 6*, 479−491.

(25) Zhou, Y., Kim, J., Yuan, X., and Braun, T. (2011) Epigenetic modifications of stem cells: a paradigm for the control of cardiac progenitor cells. *Circ. Res. 109*, 1067−1081.

(26) Wen, B., Wu, H., Shinkai, Y., Irizarry, R. A., and Feinberg, A. P. (2009) Large histone H3 lysine 9 dimethylated chromatin blocks distinguish differentiated from embryonic stem cells. *Nat. Genet. 41*, 246−250.

(27) Chen, J., Liu, H., Liu, J., Qi, J., Wei, B., Yang, J., Liang, H., Chen, Y., Wu, Y., Guo, L., Zhu, J., Zhao, X., Peng, T., Zhang, Y., Chen, S., Li, X., Li, D., Wang, T., and Pei, D. (2013) H3K9 methylation is a barrier during somatic cell reprogramming into iPSCs. *Nat. Genet. 45*, 34−42.

(28) Comes, S., Gagliardi, M., Laprano, N., Fico, A., Cimmino, A., Palamidessi, A., De Cesare, D., De Falco, S., Angelini, C., Scita, G.,

DOI: 10.1021/cb5008037
ACS Chem. Biol. 2015, 10, 165−174

Patriarca, E. J., Matarazzo, M. R., and Minchiotti, G. (2013) L-Proline Induces a Mesenchymal-like Invasive Program in Embryonic Stem Cells by Remodeling H3K9 and H3K36 Methylation. *Stem Cell Rep. 1*, 307−321.

DOI: 10.1021/cb5008037
ACS Chem. Biol. 2015, 10, 165−174